Available online at www.sciencedirect.com
ScienceDirect
Metabolism Clinical and Experimental 57 (2008) 966–972
Metabolism
Clinical and Experimental
www.metabolismjournal.com

The hyperenergetic-fed obese dog, a model of disturbance of apolipoprotein B-100 metabolism associated with insulin resistance: kinetic study using stable isotopes

François Briand[a,b,1], Edwige Bailhache[a,b,1], Agnes Andre[a,c], Thierry Magot[a], Michel Krempf[a], Patrick Nguyen[b], Khadija Ouguerram[a,*]

[a]*Centre de Recherche en Nutrition Humaine, Institut national de la santé et de la recherche médicale, INSERM U539, CHU Nantes F-44000, France*
[b]*USC INRA de Nutrition et Endocrinologie, Ecole nationale vétérinaire de Nantes, CHU Nantes F-44000, France*
[c]*Physiogenex SAS, Prologue Biotech, Labege F-31000, France*

Received 17 September 2007; accepted 15 February 2008

Abstract

The hyperenergetic-fed beagle dog model of obesity-associated insulin resistance has previously demonstrated lipoprotein abnormalities similar to those of obese insulin-resistant humans. The aim of this study was to check, in the insulin-resistant dog, the mechanism leading to abnormalities in the mass of apolipoprotein B-100 (apo B-100) containing lipoproteins. Six healthy male beagle dogs were overfed with a high-fat diet for 28 ± 2.5 weeks. Obesity was associated with insulin resistance as assessed by the euglycemic hyperinsulinemic clamp technique. The kinetics of very low-density lipoprotein (VLDL) and low-density lipoprotein (LDL) apo B-100 were recorded in dogs, at healthy and insulin-resistant states, using a primed constant infusion of [5,5,5-D_3]leucine. Isotopic enrichment was measured by gas chromatography–mass spectrometry (GC-MS). A multicompartmental model was used for the analysis of tracer kinetics data. Apolipoprotein B-100 concentration was higher in VLDL (2.8-fold, $P < .05$) but lower in LDL (2-fold, $P < .05$) in the insulin-resistant compared to the healthy state. Kinetic analysis showed a higher VLDL apo B-100 production (1.7-fold, $P < .05$). The fractional catabolic rate of VLDL did not change significantly, but the lipolysis was decreased significantly (3-fold, $P < .05$). The lower LDL apo B-100 level in insulin-resistant dogs was explained by a higher LDL fractional catabolic rate (2.5-fold, $P < .05$). The mechanisms leading to hypertriglyceridemia (higher production rate and lower lipolysis of VLDL) in insulin-resistant dogs were similar to those described in the insulin-resistant humans.

It has been well demonstrated that insulin resistance and associated dyslipidemia play an important role in the progression of atherosclerosis [1]. In humans, the consumption of energy-dense/high-saturated fat diets is strongly and positively associated with overweight that, in turn, deteriorates insulin sensitivity [2]. The development of strategies to improve insulin sensitivity [3] has been facilitated since some molecular mechanisms accounting for skeletal muscle insulin resistance in type 2 diabetes mellitus were characterized [4]. Euglycemic hyperinsulinemic clamp and glucose tolerance tests [5] are 2 methods used to assess insulin resistance in humans. However, in clinical studies, it is impossible to investigate the different steps of insulin resistance development. However, it is crucial to detect insulin resistance at early stage in humans to perform adapted therapy preventing diabetes onset. The only alternative to assay insulin resistance at an early stage is the use of animal models. Many animal species may develop an insulin resistance, including hamster [6], mouse [7], and rat [8]. However, they are not perfect models because of their small size, which is not conducive to investigate the origin of dyslipidemia, especially by kinetic studies. Rodents have been studied most thoroughly because mostly of economic considerations and their short generation time that allows the study of inherited disorders. Larger animal models, such as

* Corresponding author. Tel.: +33 240087535; fax: +33 240087544.
E-mail address: khadija.ouguerram@univ-nantes.fr (K. Ouguerram).
[1] These authors participated equally to this work.

0026-0495/$ – see front matter © 2008 Elsevier Inc. All rights reserved.
doi:10.1016/j.metabol.2008.02.013

pig [9], have also been developed. In our laboratory, we have recently developed an insulin-resistant dog model induced by an hyperenergetic diet exhibiting plasma lipid disorders [10]. Insulin-resistant dogs have high triglyceride and nonesterified fatty acid (NEFA) levels, as well as low high-density lipoprotein (HDL) cholesterol levels, which are the most common abnormalities in insulin-resistant humans [11]. The impact of insulin resistance was investigated on HDL metabolism in this animal model demonstrating a decrease in reverse cholesterol transport intensity [12]. Studies in insulin-resistant humans have shown that hypertriglyceridemia is related to a high very low-density lipoprotein (VLDL) production and delayed VLDL catabolism [13]. In insulin-resistant animals [14,15], a higher VLDL production has been reported using triton, which inhibits the VLDL conversion. With this technique, unlike isotope studies, only VLDL accumulation can be measured. Indeed, in these small animal models, integrated kinetic studies, including the relationships between lipoproteins, are complex because the volume of blood samples is limited. A large animal such as the dog is a much more suitable model to elucidate mechanisms inducing lipoprotein metabolism disturbance observed in insulin-resistant states. In this study, the kinetics of apo B-100–containing lipoproteins were conducted in the same dogs before and after they became insulin-resistant.

1. Materials and methods

1.1. Animals and diet

All dogs were housed according to the regulations for animal welfare of the French Ministry of Agriculture and Fisheries. The experimental protocols adhered to European Union guidelines and were approved by the Animal Use and Care Advisory Committee of the University of Nantes. Only healthy animals were enrolled: hematocrit of more than 38%, leukocyte count of less than 18 000/mm^3, good appetite, no medications, and normal stools. Healthy dogs consumed in a single meal a dry commercial dog food (27% crude protein, 13% ether extract, 3730 kcal metabolizable energy per kilogram, on a dry matter basis) and were fed according to the National Research Council recommendation (132 kcal metabolizable energy per kilogram of body weight $[BW]^{0.75}$). Ten healthy adult male beagle dogs were randomly divided into 2 groups. Four dogs, the control group for aging, were fed with the commercial diet. The 6 other dogs (BW, 12.1 ± 0.9 kg; age, 4.1 ± 0.9 years) were submitted to hyperenergetic and hyperlipidemic diet to induce obesity. These dogs were given, ad libitum, a hyperenergetic diet comprising 75% of the energy allowance from a dry diet (34% crude protein, 32.6% ether extract, 4790 kcal metabolizable energy per kilogram, on a dry matter basis) and 25% from a canned diet (35% crude protein, 20% ether extract, 3860 kcal metabolizable energy per kilogram, on a dry matter basis). Intake of each diet was recorded daily.

1.2. Assessment of insulin sensitivity

Insulin sensitivity was assessed using the euglycemic hyperinsulinemic clamp technique [16] in conscious dogs, before weight gain and when BW gain had been at least 20% of initial BW. All experiments were performed on dogs after stabilization of body weight during at least 5 weeks.

1.3. Leucine

[5,5,5-D_3]leucine (≥98% atom D) was obtained from Eurisotop (Gif-sur-Yvette, France). Tracer solution was determined to be sterile (plate culture) and 98% or more chemically and optically pure before use. Stable isotope tracer was weighed on a high-precision scale and dissolved in known volumes of sterile 0.9% NaCl. Solutions were prepared the day of the study.

1.4. Kinetic study

The kinetic study was performed in 6 dogs at healthy and obese state. Animals were unfed for 20 hours before the beginning of the experiment and during the entire protocol. However, they were always given access to water. Two intravenous catheters were inserted: the first one (Vasocan Braunüle, 20G 1 1/4″, Melsungen, Germany) in the cephalic vein of a forelimb for infusion of [5,5,5-D_3]leucine and the second one (Vygon 20G 8cm, Ecouen, France) in a jugular vein for collection of blood samples. Animals were not anesthetized during the entire experiment. During the perfusion, dogs can move freely in their cage. Each animal received intravenously a prime of 10 μmoL/kg of tracer, immediately followed by a constant tracer infusion (10 μmoL/kg per hour) for 8 hours. Venous blood samples (10 mL each) were withdrawn in EDTA tubes (Venoject, Paris, France) at baseline, every 15 minutes during the first hour and then regularly until the end of the infusion. Six blood samples were collected during the 18 hours after the end of the infusion. Plasma was immediately separated by centrifugation at 5000 rpm for 10 minutes at 4°C. Sodium azide, an inhibitor of bacterial growth, and Pefabloc SC (Interchim, Montluçon, France), a protease inhibitor, were added to plasma samples that were frozen at −80°C until analysis.

1.5. Analytical procedures

Very low-density lipoproteins were isolated by standard ultracentrifugation methods [17] using a fixed angle rotor at 40 000 rpm for 22 hours at 4°C (Himac CP 70, Hitachi, Hialeah, FL). Four-milliliter plasma samples were overlaid with 2.5 mL of 0.9% NaCl containing 2 mmol/L EDTA (density, 1.006 g/mL) before centrifugation. The VLDL fraction was removed in the top 1.5 mL. Because a fraction of the low-density lipoproteins (LDLs) have the same density as some high-density lipoproteins (HDL) in dogs [18], another method of separation was necessary. Low-density lipoproteins were precipitated from the infranatant by the addition of 5 mL of 101 mmol/L heparin manganese

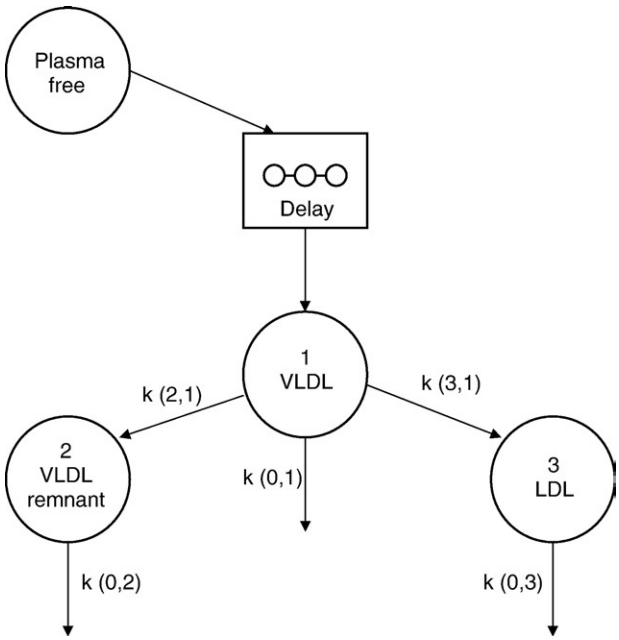

Fig. 1. Model of apo B-100 metabolism in dogs. Precursor pool was represented by plasma free leucine tracer-to-tracee ratios as forcing function. "Delay" indicates the time required for apo B-100 secretion into lipoproteins; compartment 1, VLDL-apo B-100; compartment 2, VLDL remnant-apo B-100; compartment 3, LDL-apo B-100.

chloride, followed by incubation for 30 minutes and then centrifuged at 4000 rpm, 4°C, for 30 minutes [19]. The LDL precipitate was resolubilized with 0.25 mL 0.5 mol/L sodium citrate and 1 mL 0.15 mol/L sodium chloride and then dialyzed overnight at 4°C against sodium chloride/azide (8.77 g sodium chloride, 0.13 g sodium nitrite, 0.372 g Na_2EDTA in 1 L, pH 7.3).

Apolipoprotein B-100 was isolated from VLDL and LDL by preparative sodium dodecyl sulfate polyacrylamide gel electrophoresis using a 4% stacking and a 10% resolving. Gels were stained in a solution of 0.02% Coomassie blue, 25% methanol, 10% acetic acid, and were destained with frequent changes of 10% acetic acid until the background was clear. Apolipoproteins were identified by comparing migration distances with those of standards of known molecular weight. The band of apo B-100 was excised from the stained gel and hydrolyzed in 4N HCl at 110°C for 24 hours. The hydrolyzate was evaporated under nitrogen and 1 mL of 1N acetic acid was added to each vial. Amino acids were isolated using Dowex 50WX8-200 cation exchange resin (Biod-Rad Labs, Richmond, CA), esterified with propanol/acetyl chloride, and further derivatized using heptafluorobutyric anhydride (Fluka Chemie AG, Buchs, Switzerland) before analysis.

For plasma leucine analysis, samples (100 μL) were buffered with 1 mL of 1N acetic acid, and the same procedure for hydrolysis, cation exchange chromatography, and derivatization (described above) was undertaken.

Apolipoprotein B-100 concentration was obtained in lipoprotein fractions using the isopropanol precipitation method [20]. The leucine content in precipitated apo B-100 was determined using norleucine as internal standard [21]. A constant amount of norleucine (46 nmol) was added to precipitated apo B-100, and the same procedure was undertaken for hydrolysis, cation exchange chromatography, and derivatization as described above. By mass spectrometry, the ratio of leucine ion abundance was used to determine the quantity of leucine in the sample by comparison to a standard curve containing different amounts of leucine (0-200 μmol) and a constant amount of norleucine (6 μmol). The corresponding amount of apo B-100 was then calculated according to the number of leucine molecules per apo B-100 molecule [22].

1.6. Determinations of tracer-to-tracee ratios

Chromatographic separations were carried out on a 30-m × 0.25-mm × 0.25-μm DB-1 capillary column (J & W Scientific, Rancho Cordova, CA). The column temperature program was as follows: initial temperature was held at 70°C, increased by 10°C per minute to an intermediate temperature of 170°C and then increased by 40°C per minute to a final temperature of 250°C. Electron impact gas chromatography-mass spectrometry (GC-MS) was performed on a 5891 A gas chromatograph connected to a 5971 A quadrupole mass spectrometer (Hewlett-Packard, Palo Alto, CA). The isotopic ratio was determined by selected ion monitoring at m/z 282 and 285. Calculations of apo B-100 kinetic parameters were based on the tracer-to-tracee mass ratio [23].

1.7. Modeling

Tracer-to-tracee ratios of apo B-100 leucine in VLDL and LDL were analyzed by multicompartmental modeling. The SAAM II program was used to fit the model to the observed tracer data by a weighed-least-squares approach to find the best fit as previously described [24] and to determine the parameters of the model (SAAM II v 1.0.1, Resource Facility for Kinetic Analysis, Department of Bioengineering, SAAM Institute, Seattle, WA). Implicit in the use of this model is the assumption that each animal remains in steady state with respect to their apo B-100 metabolism during the time course of the study.

The model used for healthy and insulin-resistant dogs consisted of 3 compartments (Fig. 1), as previously described [25]. Briefly, tracer-to-tracee ratio of plasma free leucine was used as a forcing function describing the input of labeling into the system. Compartment 1 represents VLDL-apo B-100, compartment 2 VLDL remnant-apo B-100, and compartment 3 LDL-apo B-100. In this model, LDL production only arises from VLDL lipolysis.

Because of the heterogeneity of VLDL, parameters of VLDL direct removal and lipolysis were calculated as follows from rate constants identified using the model:

M_1 is apo B-100 concentration in VLDL and M_2 is apo B-100 in VLDL remnant.

Table 1
Clinical and biological characteristics of studied animals

Parameter	Control state	Insulin-resistant state
Weight (kg)	12.1 ± 0.9	18.1 ± 1.8 *
Fasting blood glucose (mg/dL)	83 ± 3	89 ± 2
Fasting insulin (μU/mL)	10 ± 2	24 ± 4 *
Glucose infusion rate (mg/kg per minute)	28.1 ± 2.8	15.3 ± 1.2 *
Fasting triglycerides (mmol/L)	0.23 ± 0.04	0.77 ± 0.27 *
Total cholesterol (mmol/L)	5.31 ± 0.26	4.94 ± 0.31
HDL cholesterol (mmol/L)	4.78 ± 0.21	4.25 ± 0.20 *
NEFA (mmol/L)	0.984 ± 0.111	1.585 ± 0.127 *
Apo B-100 (mg/L)	386 ± 84	216 ± 63 *

* $P < .05$.

Rate constant of direct VLDL removal = $[M_1k(0,1) + M_2k(0,2)]/(M_1 + M_2)$

Rate constant of VLDL conversion rate = $M_1k(3,1)/(M_1 + M_2)$

Total VLDL apo B-100 fractional catabolic rate (FCR) is the sum of direct VLDL removal and VLDL conversion rate.

The FCR of LDL-apo B-100 corresponds to the rate constant of removal of LDL from plasma, $k(0,3)$. The apo B-100 absolute production rate (APR), in milligrams per kilogram per hour, was calculated as previously described for humans [26]. Plasma volume was estimated at 4.5% of body weight [27].

1.8. Chemical analysis

Blood glucose concentration was determined with a glucose oxidase method. Insulin was measured by radioimmunoassay on each blood sample (RIA Insik-5, Sorin Biomedica, Sorin, Italy). Triglycerides, cholesterol, and NEFA were analyzed using enzymatic methods (cholesterol RTU, BioMerieux, Marcy-l'Etoile, France; Triglycerides enzymatiques PAP 150, BioMerieux, Marcy-l'Etoile, France; NEFA C, WAKO, Oxoid, Dardilly, France).

1.9. Statistical analysis

Goodness of fit was assessed using the run test [28]. Moreover, we tested several models, and we compared all models among themselves using the Akaike's information criterion (AIC) test [29] and the F test [30]. Data are reported as means ± SD. Statistical analysis using the Instat Software package (GraphPad, San Diego, CA) was performed with the Wilcoxon paired test to determine significant differences between parameters in healthy and obese dogs. A 2-sided P value of less than .05 was considered significant.

2. Results

2.1. Control group for aging

After 28 weeks on control diet, the 4 dogs exhibited no significant change in the studied clinical characteristics: body weight (12.6 ± 0.4 vs 13.5 ± 0.8 kg), cholesterol (5.13 ± 0.22 vs 5.23 ± 0.48 mmol/L), triglycerides (0.25 ± 0.04 vs 0.26 ± 0.05 mmol/L), and total plasma apo B-100 (372 ± 41 vs 374 ± 35 mg/L), respectively, in dogs at the beginning of the study and 28 weeks later.

2.2. Insulin-resistant dog characteristics

Table 1 show the clinical and biochemical characteristics of dogs before and after weight gain. Body weight increased (1.5-fold, $P < .02$), from 12.1 ± 0.9 to 18.1 ± 1.8 kg in 28 ± 2.5 weeks (+1.3% per week). The euglycemic hyperinsulinemic clamp technique was applied to assess the insulin resistance in the dogs. The obese dogs showed significantly elevated fasting insulin concentrations (2.4-fold, $P < .05$) with no change in plasma glucose between the 2 states. The glucose uptake under hyperinsulinemia (glucose infusion rate measured during euglycemic hyperinsulinemic clamp) decreased significantly in obese dogs (28.1 ± 2.8 to 15.3 ± 1.2 mg/kg per minute, $P < .05$). Obese insulin-resistant dogs had significantly higher plasma triglycerides (2.3-fold, $P < .05$) and nonesterified fatty acids levels (1.6-fold, $P < .05$) but lower HDL cholesterol levels (1.1-fold, $P < .05$) and

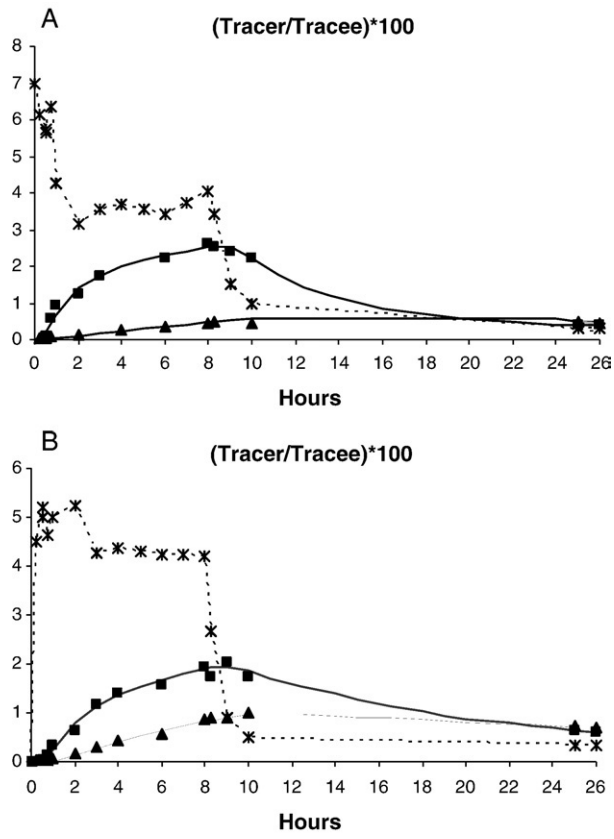

Fig. 2. Experimental values (symbols) and calculated fits (lines) of the tracer-to-tracee ratio for plasma leucine (∗), VLDL-apo B-100 (■), and LDL-apo B-100 (▲) using a 3-compartment model (see Fig. 1) for dog IV in healthy (A) and insulin-resistant state (B). Dashed lines represent forcing function (plasma leucine).

Table 2
Kinetic data of apo B-100–containing lipoproteins in control and insulin-resistant states

Dogs	VLDL apo B-100				LDL apo B-100		
	Concentration (mg/L)	APR (mg/kg per hour)	CR (h^{-1})	FCR (h^{-1})	Concentration (mg/L)	APR (mg/kg per hour)	FCR (h^{-1})
C-I	8.88	1.05	1.38	2.64	695	0.55	0.018
C-II	11.1	0.39	0.47	0.77	181	0.24	0.029
C-III	8.67	0.94	2.34	2.38	558	0.91	0.036
C-IV	13.5	0.75	0.67	1.22	340	0.41	0.027
C-V	7.3	0.35	0.73	1.06	210	0.24	0.025
C-VI	6.88	0.45	0.69	1.46	269	0.21	0.017
Mean ± SD	9.39 ± 2.50	0.66 ± 0.30	1.05 ± 0.71	1.59 ± 0.75	375 ± 206	0.43 ± 0.27	0.025 ± 0.007
IR-I	32	1.25	0.39	0.87	510	0.56	0.024
IR-II	21.1	2.41	0.45	2.41	116	0.43	0.082
IR-III	22.2	1.13	0.43	1.12	122	0.43	0.078
IR-IV	40	0.8	0.09	0.44	120	0.26	0.048
IR-V	19.8	0.41	0.29	0.46	167	0.26	0.035
IR-VI	22	0.74	0.56	0.75	115	0.55	0.106
Mean ± SD	26.18 ± 8.06 *	1.12 ± 0.70 *	0.37 ± 0.16 *	1.01 ± 0.73	191.7 ± 157.2 *	0.42 ± 0.13	0.062 ± 0.031 *

C indicates control; IR, insulin-resistant; CR, conversion rate.
* $P < .05$.

lower plasma apo B-100 concentrations (1.8-fold, $P < .05$) compared to the lean state.

2.3. Kinetic data

Glycemia, plasma triglycerides, and apo B-100 were controlled during the entire study to ensure that dogs were investigated under steady-state conditions. No change was observed for these parameters (data not shown). Tracer/tracee curves of one representative dog are shown in Fig. 2. Model fitted lines and experimental points showed close agreement, and the masses of apo B-100 calculated by this model in each compartment were not significantly different from chemically measured values (data not shown). The individual and mean kinetic parameters of VLDL and LDL apo B-100 are presented in Table 2. Apolipoprotein B-100 concentration in VLDL was significantly increased (2.8-fold, $P < .05$). Very low-density lipoprotein production was increased (1.7-fold, $P < .05$) in the insulin resistance state. Moreover, we observed a major decrease (3-fold, $P < .05$) in the conversion rate of VLDL into LDL (from 1.05 ± 0.71 to 0.37 ± 0.16 per hour) with insulin resistance with no change in their FCR. Then, the proportion of the VLDL apo B-100 cleared was, respectively, about 20% through the VLDL remnants and direct removal and 60% toward LDL in control state (data not shown). During insulin resistance state, these values were 30% and 40%, respectively, through these 2 pathways. Data on LDL showed a decrease (2-fold, $P < .05$) in apo B-100 concentration with insulin resistance. This apo B-100 decrease was accompanied with a significant increase in the FCR (2.5-fold, $P < .05$). The APR of LDL remained unchanged.

3. Discussion

This study was designed to explore the metabolism of apo B-100 in insulin-resistant dogs, using endogenous labeling with stable isotopes combined with compartmental modeling. The hyperenergetic diet resulted in obesity and insulin resistance in all dogs. Our data showed that compared to control dogs, insulin-resistant dogs exhibited higher triglyceride levels related to an increased VLDL concentration. The higher VLDL apo B-100 content can be explained by a higher VLDL production rate. The lower LDL apo B-100 concentration is partly linked to the higher FCR.

These results are consistent with data from previous researches conducted both in vitro and in vivo. Indeed, in rat hepatocytes, it has been shown that insulin inhibits apo B-100 secretion by stimulating the degradation of newly synthesized apo B-100 [31]. The increased intracellular stability of nascent apo B-100 and enhanced expression of microsomal transfer protein (MTP) would facilitate the assembly and secretion of apo B-100–containing lipoprotein particles shown in insulin resistance states [32]. In animal models, the hepatic VLDL apo B overproduction was directly associated with attenuated hepatic insulin signaling and insulin resistance [15]. A higher VLDL level in the pre–insulin-resistant Otsuka Long-Evans Tokushima Fatty rat was also associated with a higher expression of both acyl coenzyme A synthase and MTP genes [33]. Likewise, MTP activity and in vivo triglycerides secretion were enhanced in the fructose-fed hamster model [34]. In addition, NEFA influx in the liver increases triglycerides intracellular availability and provides lipid substrate for MTP activity and VLDL assembly [14]. In the present study, VLDL-apo B-100 overproduction in insulin-resistant dogs could result from impaired action of insulin.

The decrease in VLDL conversion rate observed in our study has also been reported in the literature in subjects with type 2 diabetes mellitus [26,35]. The decrease in lipoprotein lipase (LPL) activity has been shown to result in a normal [26] or a lower [13] FCR of VLDL. Our results showed a nonsignificant decrease in this value. The explanation of this

lower conversion rate may be the decreased abundance of active LPL on endothelial surfaces [28]. Indeed, it was demonstrated that LPL activity was increased after 4 months in patients with type 2 diabetes mellitus on insulin therapy [36,37]. The analysis of VLDL apo B-100 channeling through different pathways (VLDL remnant, VLDL direct removal, and conversion to LDL) showed that the decrease of lipolysis in this study led to a lower proportion of VLDL apo B cleared through LDL pathway in insulin resistance state compared to control dogs (~40% vs 60%). This channeling disturbance is in accordance with previously published data in insulin-resistant human compared to control subjects (~40% vs 80%) [26].

In our study, insulin-resistant dogs exhibited significantly lower LDL apo B-100 concentration and higher LDL FCR compared to the normal state. In humans, despite the higher concentration of VLDL, the amount of LDL reported in insulin-resistant patients has been inconsistent with normal [38], occasionally more than [26] or even lower [39] than the current National Cholesterol Education Program–recommended values [40]. In the same way, insulin-resistant dogs showed a higher VLDL concentration and a lower LDL concentration. Low-density lipoprotein kinetics data on insulin-resistant subjects were variable. On one hand, a lower LDL production rate and a higher LDL FCR have been reported in insulin-resistant subjects with a low LDL concentration [41]. On the other hand, insulin-resistant subjects with a normal LDL pool size, a higher APR, a higher FCR and a lower conversion of VLDL to LDL were noted [13]. Moreover, a higher LDL production and a lower catabolic rate of LDL apo B-100 were reported in another study on insulin-resistant patients [42]. In contrast, data from subjects in an early stage of insulin resistance showed a higher LDL production while the FCR was unchanged [38]. These apparent inconsistencies should result from varying levels of insulin resistance, leading to different metabolic profiles. Such discordance underlines the necessity of an animal model to investigate the different steps of insulin resistance development. In our study, the dogs fed the hyperenergetic diet were carefully monitored, and lipoprotein investigations started as soon as insulin resistance associated with hypertriglyceridemia occurred. Thus, the tendency to a low LDL level observed in the present study could be specific to an early stage in the time course of insulin resistance.

Because it exhibited enhanced VLDL apo B-100 production and reduced lipolysis, our dog model could be very useful to investigate the different steps in the time course of insulin resistance. It could also be interesting to test different pharmacologic and nutritional treatments allowing the prevention or the reversibility of insulin resistance.

References

[1] Bamba V, Rader DJ. Obesity and atherogenic dyslipidemia. Gastroenterology 2007;132:2181-90.

[2] Riccardi G, Giacco R, Rivellese AA. Dietary fat, insulin sensitivity and the metabolic syndrome. Clin Nutr 2004;23:447-56.

[3] Li J, Tian H, Li Q, et al. Improvement of insulin sensitivity and beta-cell function by nateglinide and repaglinide in type 2 diabetic patients—a randomized controlled double-blind and double-dummy multicentre clinical trial. Diabetes Obes Metab 2007;9:558-65.

[4] Karlsson HK, Zierath JR. Insulin signaling and glucose transport in insulin resistant human skeletal muscle. Cell Biochem Biophys 2007; 48:103-13.

[5] Trout KK, Homko C, Tkacs NC. Methods of measuring insulin sensitivity. Biol Res Nurs 2007;8:305-18.

[6] Leung N, Naples M, Uffelman K, et al. Rosiglitazone improves intestinal lipoprotein overproduction in the fat-fed Syrian Golden hamster. An animal model of nutritionally-induced insulin resistance. Atherosclerosis 2004;174:235-41.

[7] Nandi A, Kitamura Y, Kahn CR, et al. Mouse models of insulin resistance. Physiol Rev 2004;84:623-47.

[8] Tofovic SP, Jackson EK. Rat models of the metabolic syndrome. Methods Mol Med 2003;86:29-46.

[9] Xi S, Yin W, Wang Z, et al. A minipig model of high fat/high-sucrose diet-induced diabetes and atherosclerosis. Int J Exp Pathol 2004;85: 223-31.

[10] Bailhache E, Nguyen P, Krempf M, et al. Lipoproteins abnormalities in obese insulin-resistant dogs. Metabolism 2003;52:559-64.

[11] Chahil TJ, Ginsberg HN. Diabetic dyslipidemia. Endocrinol Metab Clin North Am 2006;35:491-510.

[12] Briand F, Bailhache E, Nguyen P, et al. Metabolism of high density lipoprotein apolipoprotein A-I and cholesteryl ester in insulin resistant dog: a stable isotope study. Diabetes Obes Metab 2007;9:139-42.

[13] Kissebah AH, Alfarsi S, Evans DJ, et al. Integrated regulation of VLDL triglyceride and apolipoprotein B kinetics non–insulin-dependant diabetes mellitus. Diabetes 1982;31:217-24.

[14] Zoltowska M, Ziv E, Delvin E, et al. Both insulin resistance and diabetes in *Psammomys obesus* upregulate the hepatic machinery involved in intracellular VLDL assembly. Arterioscler Thromb Vasc Biol 2004;24:118-23.

[15] Haidari M, Leung N, Mahbub F, et al. Fasting and postprandial overproduction of intestinally derived lipoproteins in an animal model of insulin resistance. Evidence that chronic fructose feeding in the hamster is accompanied by enhanced intestinal de novo lipogenesis and apoB48-containing lipoprotein overproduction. J Biol Chem 2002; 277:31646-55.

[16] Bailhache E, Ouguerram K, Gayet C, et al. An insulin-resistant hypertriglyceridaemic normotensive obese dog model: assessment of insulin resistance by the euglycaemic hyperinsulinaemic clamp in combination with the stable isotope technique. J Anim Physiol Anim Nutr 2003;87:86-95.

[17] Havel RJ, Eder A, Bragdon JH. The distribution and chemical composition of ultracentrifugally separated lipoproteins in human serum. J Clin Invest 1955;34:1345-53.

[18] Mahley RW, Weisgraber KH. Canine lipoproteins and atherosclerosis. I. Isolation and characterization of plasma lipoproteins from control dogs. Circ Res 1974;35:713-21.

[19] Barrie J, Nash AS, Watson TDG. Quantitative analysis of canine plasma lipoproteins. J Small Anim Pract 1993;34:226-31.

[20] Egusa G, Brady DW, Grundy SM, et al. Isopropanol precipitation method for the determination of apolipoprotein B specific activity and plasma concentrations during metabolic studies of very low density lipoprotein and low density lipoprotein apolipoprotein B. J Lipid Res 1983;24:1261-7.

[21] Beghin L, Duhal N, Poulain P, et al. Measurement of apolipoprotein B concentration in plasma lipoproteins by combining selective precipitation and mass spectrometry. J Lipid Res 2000;41:1172-6.

[22] Yao Z, McLeod RS. Synthesis and secretion of hepatic apolipoprotein B–containing lipoproteins. Biochim Biophys Acta 1994;1212:152-66.

[23] Cobelli C, Toffolo G, Bier DM, et al. Models to interpret kinetic data in stable isotope tracer studies. Am J Physiol 1987;253:551-64.

[24] Maugeais C, Ouguerram K, Krempf M, et al. Kinetic study of apo B100 containing lipoprotein metabolism using amino acids labeled with stable isotopes: methodological aspects. Clin Chem Lab Med 1998;36:739-45.
[25] Bailhache E, Briand F, Nguyen P, et al. Metabolism of cholesterol ester of apolipoprotein B100–containing lipoproteins in dogs: evidence for disregarding cholesterol ester transfer. Eur J Clin Invest 2004;34: 527-34.
[26] Ouguerram K, Magot T, Zair Y, et al. Effect of atorvastatin on apolipoprotein B100 containing lipoprotein metabolism in type-2 diabetes. J Pharmacol Exp Ther 2003;306:332-7.
[27] Swanson KS, Kuzmuk KN, Schook LB, Fahey Jr GC. Diet affects nutrient digestibility, hematology, and serum chemistry of senior and weanling dogs. J Anim Sci 2004;82:1713-24.
[28] Sokal RR, Rohlf FJ. Miscellaneous methods. In: Freeman WH, editor. Biometry. The principles and practice of statistics in biological research. 3rd ed. New York: Freeman; 1995. p. 797-803.
[29] Akaike H. A new look at the statistical model identification. IEEE Trans Automat Contr AC 1974;19:710-6.
[30] Boxenbaum HG, Tiegelman N, Elastoff RM. Statistical estimation in pharmacokinetics. J Pharmacokinet Biopharm 1974;2:123-48.
[31] Sparks JD, Sparks CE. Insulin modulation of hepatic synthesis and secretion of apolipoprotein B by rat hepatocytes. J Biol Chem 1990; 265:8854-62.
[32] Zoltowska M, Ziv E, Delvin E, et al. Cellular aspects of intestinal lipoprotein assembly in *Psammomys obesus*: a model of insulin resistance and type 2 diabetes. Diabetes 2003;52:2539-45.
[33] Kuriyama H, Yamashita S, Shimomura I, et al. Enhanced expression of hepatic acyl-coenzyme A synthetase and microsomal triglyceride transfer protein messenger RNAs in the obese and hypertriglyceridemic rat with visceral fat accumulation. Hepatology 1998;27: 557-62.
[34] Taghibiglou C, Carpentier A, Van Iderstine SC, et al. Mechanisms of hepatic very low density lipoprotein overproduction in insulin resistance: evidence for enhanced lipoprotein assembly. Reduced intracellular ApoB degradation. and increased microsomal triglyceride transfer protein in a fructose-fed hamster model. J Biol Chem 2000; 275:8416-25.
[35] Taskinen MR, Packard CJ, Shepherd J. Effect of insulin therapy on metabolic fate of apolipoprotein-B containing lipoproteins in NIDDM. Diabetes 1990;39:1017-27.
[36] Simsolo RB, Ong JM, Saffari B, et al. Effect of improved diabetes control on the expression of lipoprotein lipase in human adipose tissue. J Lipid Res 1992;33:89-95.
[37] Geltner C, Lechleitner M, Foger B, et al. Insulin improves fasting and postprandial lipemia in type 2 diabetes. Eur J Intern Med 2002;13: 256-63.
[38] Pont F, Duvillard L, Florentin E, et al. Early kinetic abnormalities of apoB-containing lipoproteins in insulin-resistant women with abdominal obesity. Arterioscler Thromb Vasc Biol 2002;22:1726-32.
[39] Cowie CC, Howard BV, Harris MI. Serum lipoproteins in African Americans and Whites with non–insulin-dependent diabetes in the US population. Circulation 1994;90:1185-93.
[40] Pang RW, Tam S, Janus ED, et al. Plasma lipid, lipoprotein and apolipoprotein levels in a random population sample of 2875 Hong Kong Chinese adults and their implications (NCEP ATP-III, 2001 guidelines) on cardiovascular risk assessment. Atherosclerosis 2006; 184:438-45.
[41] Howard BV, Egusa G, Beltz WF, et al. Compensatory mechanisms governing the concentration of plasma low density lipoprotein. J Lipid Res 1986;27:11-20.
[42] Chan DC, Watts GF, Redgrave TG, et al. Apolipoprotein B-100 kinetics in visceral obesity: associations with plasma apolipoprotein C-III concentration. Metabolism 2002;51:1041-6.